Electronic Supplementary Information for

Electrochemical properties of fluorinated boron-doped diamond electrodes via fluorine-containing plasma treatment

Chizu Yamaguchi,[a] Keisuke Natsui,[a] Shota Iizuka,[b] Yoshitaka Tateyama,[b] and Yasuaki Einaga*[ac]

[a]Department of Chemistry, Keio University, 3-14-1 Hiyoshi, Yokohama 223-8522, Japan

[b]Center for Green Research on Energy and Environmental Materials (GREEN) and International Center for Materials Nanoarchitectonics (MANA), National Institute of Materials Science (NIMS), 1-1 Namiki, Tsukuba, Ibaraki 305-0044, Japan

[c]ACCEL, Japan Science and Technology Agency, 5-3 Yobancho, Chiyoda-ku, Tokyo 102-8666, Japan

*Corresponding author. E-mail address: einaga@chem.keio.ac.jp

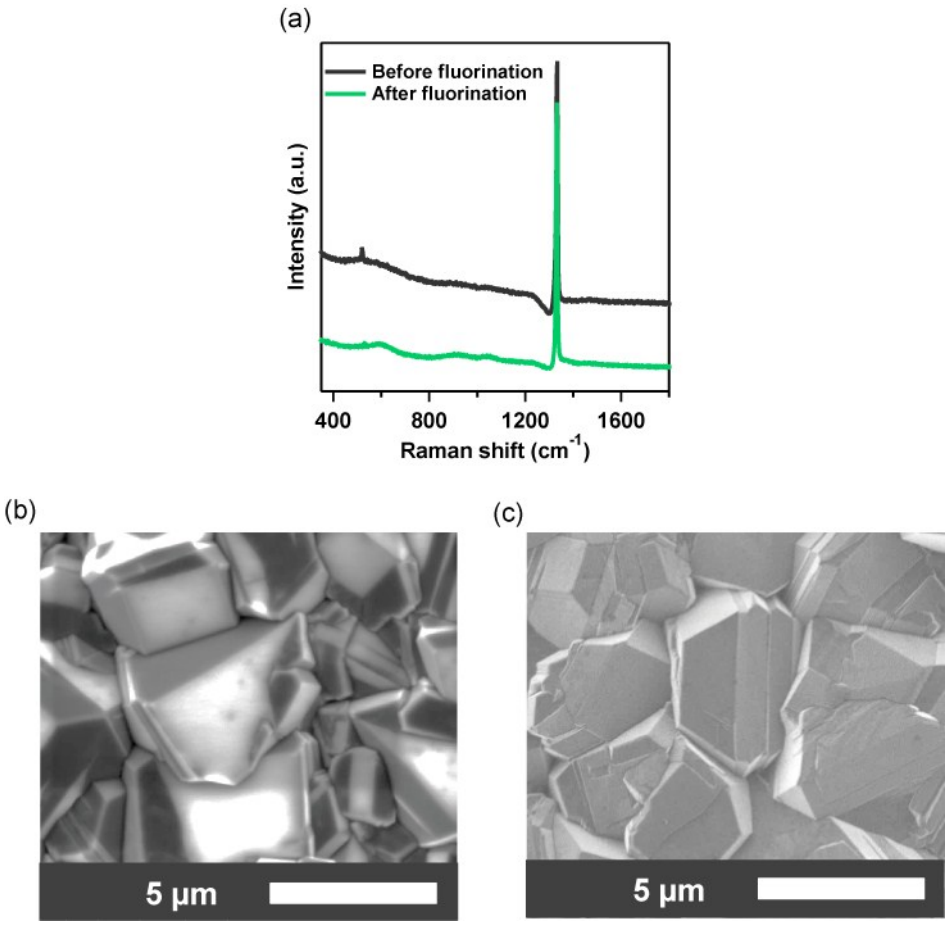

Figure S1. (a) Raman spectra of BDD before (black) and after (green) C_3F_8 plasma treatment, and SEM images of BDD before (b) and after (c) C_3F_8 plasma treatment.

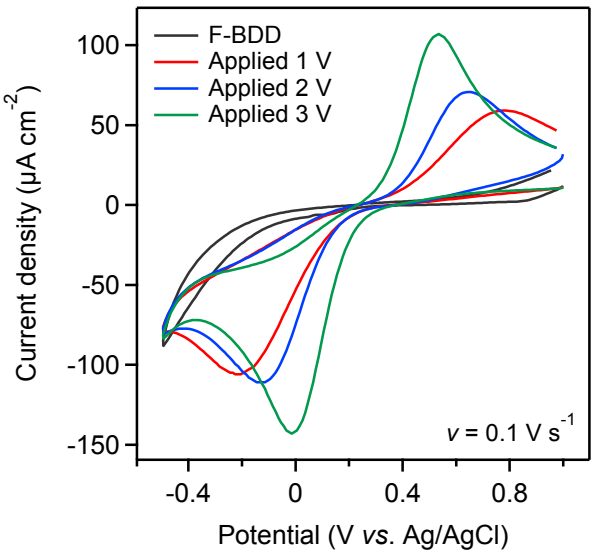

Figure S2. CVs of F-BDD after applying positive potentials in the aqueous solution of 1 mM $K_3[Fe(CN)_6]$ with 1 M KCl. 1 V (red), 2 V (blue), and 3 V (green) (versus Ag/AgCl) were applied to F-BDD in an aqueous solution of 0.1 M H_2SO_4 until ΔE_p converged at constant values. The voltammogram of F-BDD without any polarization (black) was also measured for comparison.

Table S1. Convergence Values of ΔE_p (Peak-to-Peak Potential Separation in $K_3[Fe(CN)_6]$ Aqueous Solution), Water Contact Angle (CA) Values, F/C Ratio, and O/C Ratio of F-BDD after Each Polarization.

Applied potential (*vs*. Ag/AgCl)	ΔE_p (V)	CA (°)	F/C*	O/C*
not-applied	>1.50	111.7±1.9	0.31	0.08
1 V	1.00	86.4±2.5	0.25	0.10
2 V	0.78	71.4±5.6	0.19	0.16
3 V	0.55	54.0±8.0	0.16	0.10
−1 V	0.96	85.2±7.8	0.17	0.15
−2 V	0.66	91.8±2.3	0.15	0.12
−3 V	0.49	83.2±4.1	0.15	0.08

*F/C and O/C ratios calculated by XPS data.

Table S2. Water Contact Angle (CA) Values, F/C Ratio, and O/C Ratio of H-, O-, F-, and FO-BDD.

Surface Termination	CA (°)	F/C*	O/C*
H-BDD	100.3±1.7	0.0	0.03
O-BDD	35.4±2.7	0.0	0.13
F-BDD	111.7±1.9	0.31	0.08
FO-BDD	71.4±5.6	0.19	0.16

*F/C and O/C ratios calculated by XPS data.

Theoretical Calculations

We carried out density functional theory (DFT) based molecular dynamics simulations of the water interfaces with H-terminated, OH-terminated, and F-terminated BDD electrodes. Generalized gradient approximation (GGA) with Perdew-Burke-Ernzerhof (PBE) exchange−correlation energy functional[1] and Goedecker-type pseudopotentials[2,3] were used. We utilized the cutoff energy of 90 Ry for the plane wave basis set, and the Γ point sampling was used for the k-point sampling for the supercell.

The supercell with the dimensions of 10.109 x 8.755 x 54.6 $Å^3$ was used for all the systems (Figure S3). The lateral dimensions were optimized under the present calculation conditions, which gives C-C bond length of 1.55 Å. The supercell involves 105 water molecules as well as 254 carbon and 2 boron atoms for a reasonable model of low-doped BDD (~0.8%). In this study, we considered the (111) surface of BDD with 4x4 sites, and both surfaces of the BDD slab were terminated with 1 monolayer of H or OH or F species, respectively. The boron positions were chosen to simulate the homogeneous distribution. The space for water in the supercell was determined to mimic the ambient conditions.

To sample dynamics of the solid-liquid interfaces, we carried out DFT molecular dynamics (MD) simulations. The time step and the fictitious mass of electron were 4.0 a.u. and 400 a.u., respectively. The temperature was set to 300 K with the Nose thermostat (with frequency 500 cm^{-1}).[4] After the equilibrations with around 3 psec, we sampled the structural data shown in Figure S4. The layered density of states depicted in Figure S5 were calculated for the selected and well-uncorrelated snapshots. All the calculations were performed using the CPMD code.[5]

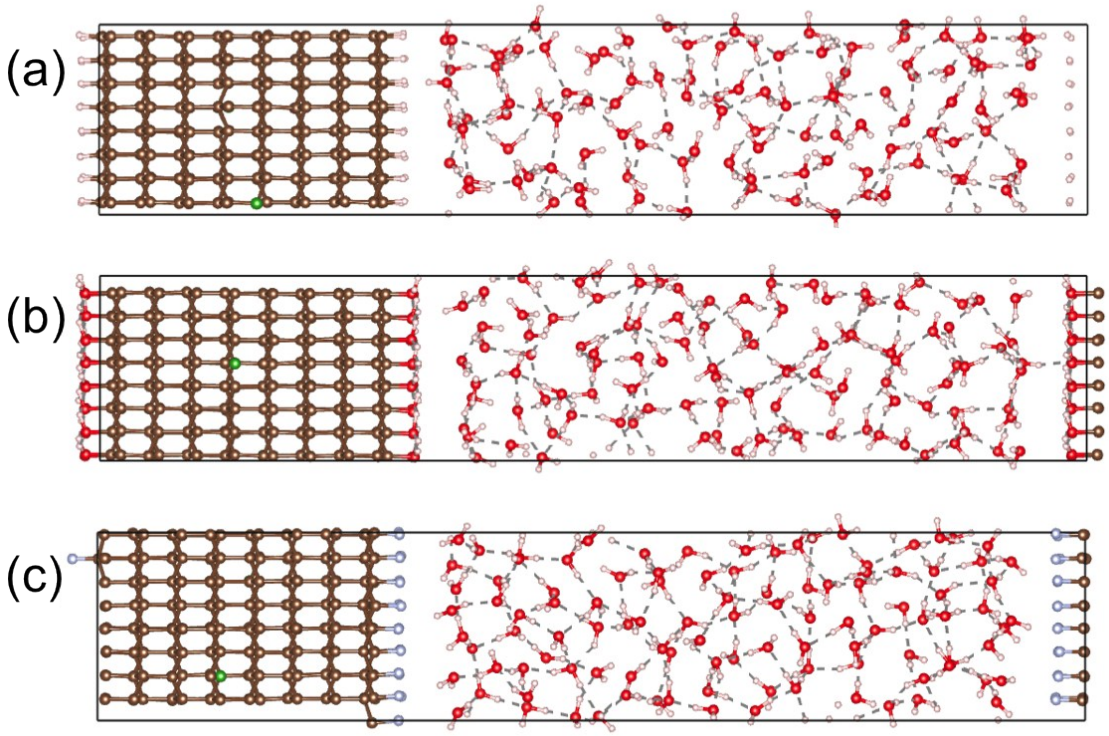

Figure S3. Snapshots of DFT molecular dynamics simulations in the supercells of (a) H-terminated BDD/water, (b) OH-terminated BDD/water, and (c) F-terminated BDD/water interfaces. The (111) facets of BDD are considered. Brown, green, red, white, and light blue spheres denote carbon, boron, oxygen, hydrogen, and fluorine, respectively.

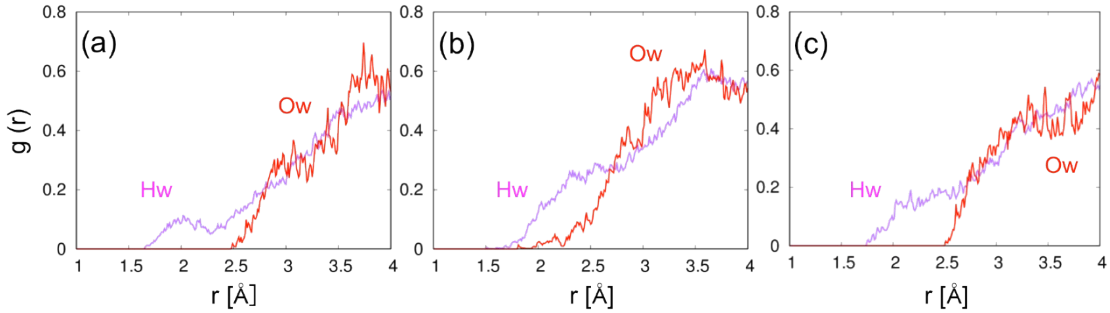

Figure S4. Radial distibution functions (RDFs), g(r), of water hydrogen (Hw: pink) and water oxygen (Ow: red) from the outermost species of (a) H-terminated BDD (H), (b) OH-terminated BDD (H), and (c) F-terminated BDD (F) at the BDD / water interfaces. For H-terminated BDD shown in (a), the Hw atoms mainly direct to the surface, and the Ow distribution appears around 2.5 Å indicating the hydrophobic situation. In (b), the Ow distribution appears around 2.0 Å suggesting that hydrogen bondings between the termination groups and interfacial water are formed and the OH-terminated BDD becomes more hydrophilic. On the other hand, for the F-terminated BDD shown in (c), the Hw and Ow distributions appear from around 1.7 and 2.5, respectively, and the number of interfacial water, estimated by the coordination numbers, looks decreasing, both of which suggest possible larger hydrophobicity for the F-terminated BDD.

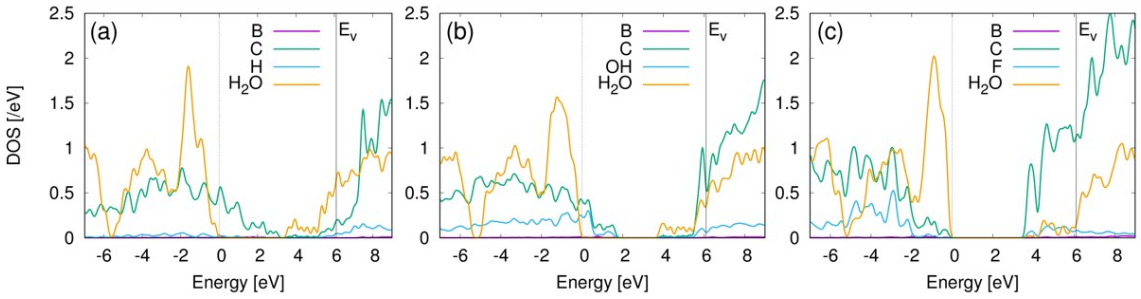

Figure S5. Projected density of states (PDOS) of the interfaces between water and (a) H-terminated BDD, (b) OH-terminated BDD, and (c) F-terminated BDD. The valence band maximum (VBM) of water is set to the energy origin. The estimated vacuum level is shown as vertical solid line (around 6 eV). The VBMs of H-BDD, OH-BDD, and F-BDD are located around 2.8 eV, 1.8 eV, and −0.2 eV, respectively. Therefore, the downward shift of BDD band is significant for F-BDD, because of the larger interfacial dipole. When the band edge pinning scheme is taken, the "interfacial" band bending is expected to be larger in F-BDD for the target redox potential, leading to suppression of interfacial electron transfer to and from this redox species in water.

References

(1) J. P. Perdew, K. Burke, and M. Ernzerhof, *Phys. Rev. Lett*., 1996, **77**, 3865.

(2) S. Goedecker, M. Teter, and J. Hutter, *Phys. Rev. B*, 1996, **54**, 1703.

(3) M. Krack, *Theor. Chem. Acc*., 2005, **114**, 145.

(4) S. Nosé, *J. Chem. Phys*., 1984, **81**, 511.

(5) CPMD V4.1. http://www.cpmd.org/, Copyright IBM Corp 1990-2015, Copyright MPI für Festkörperforschung Stuttgart 1997-2001.